European Review for Medical and Pharmacological Sciences 2020; 24: 2965-2976

Long non-coding RNA HCP5 promotes proliferation and metastasis of clear cell renal cell carcinoma *via* targeting miR-140-5p/IGF1R pathway

Y.-J. ZHANG[1], C. LU[2]

[1]Department of Urology, Dafeng People's Hospital, Dafeng, Jiangsu, China
[2]Department of Urology, Shanghai Ninth People's Hospital, School of Medicine, Shanghai Jiao Tong University, Shanghai, China

Abstract. – OBJECTIVE: The expression pattern, biological function and action mechanism of long noncoding RNA HCP5 in clear cell renal cell carcinoma (ccRCC) remain elusive.

MATERIALS AND METHODS: The quantitative Real Time-Polymerase Chain Reaction (qRT-PCR) was used to measure the abundance of HCP5 and miR-140-5p in HCC tissues and cells. Kaplan-Meier survival analysis was used to analyze the prognostic role of HCP5 for the patients. Cell proliferation, apoptosis, as well as cell cycle and metastasis were detected by CCK-8, flow cytometry, transwell migration and invasion assays, respectively. The binding sites between miR-140-5p and HCP5 or IGF1R were predicted by bioinformatic sites, and the direct interaction was confirmed by Dual-Luciferase reporter assay or RIP-ago2 assay. Western blot assay was used to detect the expression of target gene. Xenograft model was established to validate the function of HCP5 *in vivo*.

RESULTS: The expression of HCP5 was significantly upregulated in ccRCC tissues and cells. Moreover, patients with high HCP5 expression level had unfavorable overall survival (OS) and progression-free survival (PFS) compared to those with low HCP5 expression. Additionally, HCP5 knockdown led to the prohibition of ccRCC cell proliferation, colony formation, migration, and invasion; the promotion of cell cycle arrest at G0-G1 and apoptosis *in vitro*; and the inhibition of tumor growth *in vivo*. Mechanically, miR-140-5p was certified as an inhibitory target of HCP5. Furthermore, insulin-like growth factor-1 receptor (IGF1R) was identified as a direct target of miR-140-5p in ccRCC cells. Finally, we found that the inhibitory effects of the HCP5 silencing on functional behaviours were neutralized by miR-140-5p silencing.

CONCLUSIONS: HCP5 serves as a competing endogenous RNA that regulated IGF1R expression by sponging miR-140-5p in ccRCC. Hence, the HCP5/miR-140-5p/IGF1R pathway might be a promising therapeutic target in ccRCC.

Key Words:
HCP5, MiR-140-5p, IGF1R, CcRCC.

Introduction

Renal cell carcinoma (RCC) is one of the most frequent types and the second lethal malignancy among urological tumors[1]. Clear cell RCC (approximately 80-90%) is the most common pathological subtype among all RCC cases[2,3]. Surgical resection is the mainstream strategy for early stage or local advanced ccRCC, but a large number of patients still develop relapse and distant metastasis[2,3]. Currently, the drug targeted therapies, anti-angiogenic therapy and immunotherapy have provided more options for the treatment of patients with metastatic ccRCC. However, the prognosis of this disease remains poor with the median survival time of only 13 months[4]. Therefore, it is essential to figure out the molecular interactions of ccRCC tumorigenesis, and to develop better therapies for patients with this disease.

Long noncoding RNAs (lncRNAs) are transcripts longer than 200 nucleotides without the ability to encode proteins[5]; lncRNAs can exert either tumor-suppressive or oncogenic effects in tumorigenesis[6,7]. These lncRNAs functioned by sponging miRNA or mediating transcriptional and post-transcriptional modifications[6,7]. Long non-coding RNA PAXIP1-AS1 facilitated cell invasion and angiogenesis of glioma by recruiting

Corresponding Author: Chao Lu, MD; e-mail: luchao2007@126.com

transcription factor ETS1 to upregulate KIF14 expression[8]. LncRNA SNHG7 accelerated cell migration and invasion by regulating miR-34a-Snail-EMT axis in gastric cancer[9]. Long non-coding RNA CASC9 and HIF-1α formed a positive feedback loop to facilitate cell proliferation and metastasis in lung cancer[10].

LncRNA HCP5 acts as one novel oncogene to regulate the growth, metastasis and drug resistance in many cancers, such as pancreatic cancer, melanoma, breast cancer, lung cancer, thyroid cancer, colorectal cancer, osteosarcoma, cervical cancer, glioma[11-18]. Liu et al[11] demonstrated that long non-coding RNA HCP5 regulates pancreatic cancer gemcitabine (GEM) resistance by sponging hsa-miR-214-3p to target HDGF. Wei et al[12] revealed that long noncoding RNA HCP5 suppresses skin cutaneous melanoma development by regulating RARRES3 gene expression via sponging miR-12. Wang et al[13] showed that lncRNA HCP5 promotes triple negative breast cancer progression as a ceRNA to regulate BIRC3 by sponging miR-219a-5p. Jiang et al[14] showed that HCP5 is a SMAD3-responsive long non-coding RNA that promotes lung adenocarcinoma metastasis via miR-203/SNAI axis. However, the function of lncRNA HCP5 has not been investigated in ccRCC.

Also, miR-140-5p has been recognized as a tumor-suppressor in multiple cancer, such as breast cancer, gastric cancer, chronic myeloid leukemia, retinoblastoma, lung cancer[19-23]. The role of miR-140-5p has not been researched in ccRCC. Tracz et al[24] demonstrated that IGF1R exerts an oncogenic role in ccRCC tumorigenesis and progression by acting as a sponge of miRNA. However, whether miR-140-5p could inhibit ccRCC cells progression by regulating the expression of IGF1R remains elusive.

Therefore, this study's aim was to explore HCP5 expression, delineate the biological roles of HCP5, and uncover the potential mechanisms involved in ccRCC. For the first time we observed that HCP5 was significantly increased in ccRCC tissues and cells. The high expression of HCP5 was tightly related with shorter OS and PFS of patients with ccRCC. Besides, HCP5 was recognized as a competing endogenous RNA (ceRNA) for miR-140-5p. HCP5 could exert its oncogenic effects on cell growth, migration and invasion via regulating IGF1R. Overall, we firstly illuminated that HCP5 could act as an oncogene to regulate ccRCC by HCP5/miR-140-5p/IGF1R axis.

Patients and Methods

Clinical Specimens

A total of 76 paired ccRCC tissues and adjacent normal renal tissues were collected from Oct 2013 to Feb 2015 from pathological confirmed ccRCC patients who underwent surgery at Shanghai Ninth People's Hospital. All obtained specimens were instantly frozen in liquid nitrogen and preserved for RNA extraction. None of all patients received therapy such as chemotherapy, radiotherapy, targeted therapy or immunotherapy before surgical resection. The informed consents were signed by all patients for the utilization of tissue samples in research. The Ethics Committee of Shanghai Ninth People's Hospital approved this investigation.

Cell Culture

A normal human renal cell line (HK-2) and six ccRCC cell lines (786-O, Caki-2, ACHN, A498, 769P, OS-RC-2) were purchased from the National Platform of Experimental Cell Resources for Sci-Tech (Beijing, China). HK-2 cells were cultured in keratinocyte-SFM (Life Technologies, Carlsbad, CA, USA) supplemented with bovine pituitary extract (Sigma-Aldrich, St. Louis, MO, USA) and human recombinant epidermal growth factor (Gibco, Grand Island, NY, USA). Six ccRCC cell lines were cultivated in Roswell Park Memorial Institute-1640 (RPMI-1640; Life Technologies, Carlsbad, CA, USA) or Dulbecco's Modified Eagle's Medium (DMEM; Gibco, Grand Island, NY, USA) medium with 10% fetal bovine serum (FBS; Gibco, Grand Island, NY, USA), 100 U/mL penicillin, and 100 μg/mL streptomycin (Sigma-Aldrich, St. Louis, MO, USA). All the cells were maintained in humidified chamber at 37°C with 5 % CO_2.

Cell Transfection

Small interfering RNA (siRNA) against HCP5 (si-HCP5) and negative control (NC) siRNA(-si-NC) were purchased from Invitrogen (Shanghai, China). The miR-140-5p mimics, NC miRNA mimics (miR-NC), miR-140-5p inhibitor, and NC inhibitor were synthesized from Biosune Co., Ltd (Shanghai, China). Transfection was performed using lipofectamine 3000 (Thermo Fisher Scientific, Waltham, MA, USA).

RNA Extraction and RT-qPCR

TRIzol reagent (Thermo Fisher Scientific, Waltham, MA, USA) was used to isolate the total RNA of tissues or cells according to the manufacturer's protocol. Total RNA was quantified by Nan-

odrop 1000 spectrophotometer (Thermo Fisher Scientific, Waltham, MA, USA) and then the cDNA was synthesized using PrimeScrip RT Reagent Kit (TaKaRa Biotechnology Co., Ltd., Dalian, China), and subsequently, quantitative RT-PCR was performed using the SYBR Premix Ex Taq™ Kit (TaKaRa Biotechnology Co., Ltd., Dalian, China) on Roche Real-Time PCR system (LightCycler480, Roche, Basel, Switzerland) to detect the relative expression of lncRNA HCP5, miR-140-5p, IGF1R, U6 and GAPDH. All primers were shown as follows: HCP5, forward: 5'-CCGCTGGTCTCTGGACACATACT-3', reverse 3'-CTCACCTGTCGTGGGATTTTGC-5'; miR-140-5p, forward: 5'-CCAGTGCAGGGTCCGAGGT-3'; reverse, 5'-GATCCGAAACCCAGCAGACAATGTAGCTTT TTT3'; GAPDH, forward: 5'-ACCATCTTCCAGGAGCGAGA-3', reverse, 5'-GACTCCACGACGTACTCAGC-3'; U6, forward: 5'-CTCGCTTCGGCAGCACA-3', reverse, 5'-AACGCTTCACGAATTTGCGT-3'. Relative expression of all gene was determined using the $2^{-\Delta\Delta Ct}$ method by normalizing to glyceraldehyde 3-phosphate dehydrogenase (GAPDH) or U6.

CCK-8 Assay

Cell proliferation was evaluated by Cell Counting Kit-8 assay (CCK-8, Dojindo Molecular Technologies, Kumamoto, Japan) according to the manufacturer's instruction. Briefly, 2×10^3 transfected cells/well were put into 96-well plates and incubated at 37°C with 5% CO_2. After the culture as the indicated time (24, 48, 72 h), 10 μL of the CCK-8 reagent was added into each well followed by incubation for 2 h at 37°C with 5% CO_2. Then, the optical density (OD) at 450 nm was determined by microplate reader (EnVision, Multimode Plate Reader, PerkinElmer, Waltham, MA, USA).

Colony Forming Assay

A total of 300 transfected cells/well were seeded in 6-well plates cells. The cells were allowed to continue to grow until visible colonies formation (>50 cells) for 10-15 days. Subsequently, the clonogenic cells were fixed, stained with 1% crystal violet, counted under Olympus microscope.

Cell Apoptosis and Cell Cycle Analysis by Flow Cytometry

For cell apoptosis, this assay was performed by an Annexin V-FITC Apoptosis Detection Kit (BD Bioscience, Franklin Lakes, NJ, USA). Cells were transfected with indicated the siRNA or corresponding negative control and incubated for 48 h. Then, the transfected cells were collected, centrifuged and stained with Annexin V-FITC and propidium iodide (PI) solution for 15 min at room temperature in the dark. Flow cytometry (FACScan; BD Biosciences, Franklin Lakes, NJ, USA) was used to measure apoptosis. For cell cycle assay, after cells were transfected and incubated for 24 h, the transfected cells were collected, washed and then fixed in 70% ethanol at 4°C for 1 h. Then, the cells were stained with PI/RNase staining solution (BD Biosciences, Franklin Lakes, NJ, USA). Flow cytometry (FACScan; BD Biosciences, Franklin Lakes, NJ, USA) was used to analyze the cell cycle.

Migration and Invasion Assay

Transwell chambers (8.0 μm pore size; Corning, Corning, NY, USA) were used to test the migration and invasion. For the migration assay, 4×10^3 transfected cells/well were plated into the upper chamber of the transwell plates with FBS-free medium. Then, the bottom chamber was filled with medium with 10% FBS as chemical attractant. After the incubation of 24 h at 37°C, the cells migrated into the lower membranes of the insert were fixed with methanol, stained with 0.5% crystal violet, and counted in three random fields under a Leica microscope (Leica, Wetzlar, Germany) with a 50 × magnification. For the invasion assay, the top chamber membrane was pre-coated with Matrigel (BD, Biosciences, Franklin Lakes, NJ, USA) and other procedures were the same as in the assay of migration.

Nuclear and Cytoplasmic Fractions

The nuclear and cytoplasm fraction of cells were isolated using the Protein and RNA Isolation System (Pierce, Thermo Scientific, Waltham, MA, USA). GAPDH was treated as the cytoplasmic control and U6 served as the nuclear marker. Later, the HCP5 of nuclear and cytoplasm fractions were determined by the qRT-PCR.

Dual-Luciferase Reporter Assay and RNA Immunoprecipitation (RIP) Assay

The wild type (Wt) and mutant type (Mut) of the full-length lncRNA HCP5 cDNA and the 3'-UTR fragments of IGF1R containing the wild-type (Wt) or mutant (Mut) were cloned into the psiCHECK-2 vector (Promega, Madison, WI, USA). These produced vectors were named as HCP5-Wt, HCP5-Mut, IGF1R-Wt and IGF1R-Mut. The indicated vectors were co-transfected with miR-140-5p mimics into ccRCC cells by Lipofectamine 2000 (Invitrogen, Carlsbad, CA, USA) and

the Luciferase activity was detected by Luciferase assay kit (Promega, Madison, WI, USA).

The binding of miR-140-5p to HCP5 was determined using the Magna RIP RNA-Binding Protein Immunoprecipitation Kit (Millipore Inc., Billerica, MA, USA) according to the manufacturer's instructions. The RNAs binding with Ago2 antibodies or IgG control were analyzed by qRT-PCR. The detailed procedures were performed according to a previously described method[25].

Western Blot Analysis

Briefly, total protein was extracted with RIP lysis buffer, separated with 10% sodium dodecyl sulfate-polyacrylamide gel electrophoresis (SDS-PAGE), and then transferred onto polyvinylidene difluoride (PVDF) membranes. Afterwards, the membranes were blocked with 5% FBS and immunoblotted with the primary antibodies. The antibodies against IGF1R (1:1000 dilution) or GAPDH (1:10000 dilution) were purchased from Cell Signaling Technology (Cell Signaling Technology, Beverly, MA, USA). GAPDH was used as an internal control. The detailed procedures of Western blot analysis were the same as for the previously described method[26].

Animal Experiments

Twelve (6 nude mice in each group) female athymic BALB/c nude mice (four weeks old) were purchased from Model Animal Research Center of Nanjing University and feed in a SPF environment. 786-O cell (2×10^6 cells suspension in 0.1 ml PBS) transfected with si-HCP5 or si-NC were implanted subcutaneously into nude mice. The tumor size and weight were monitored once every three days until the mice were resected at 35 days after tumor inoculation. Animal studies were reported in compliance with the Arrive Guidelines.

Statistical Analysis

The data were expressed as mean ± SD for continuous variables. Statistical analysis and plots were performed using GraphPad Prism 6.0 (GraphPad Software, Inc, CA, USA). The differences between the clinical characteristics and lncRNA HCP5 expression were assessed by Chi-Square (χ^2) tests. Unpaired Student's *t*-test or one-way analysis of variance was used to compare two-group or inter-group differences. Survival analysis was performed using the Kaplan-Meier method with the log-rank test applied for comparison. The Spearman's rank test was used to determine the relationship between miR-140-5p and lncRNA HCP5 or IGF1R. The $p<0.05$ was considered to indicate a statistically significant difference.

Results

LncRNA HCP5 Was Significantly Upregulated in CcRCC and Associated with Poor Prognosis

As shown in Figure 1A, the data from bioinformatic website-"GEPIA" (http://gepia.cancer-pku.cn/) showed that lncRNA HCP5 was sharply augmented compared to normal tissues ($p<0.05$) . Then, we detected HCP5 expression in 76 pairs of ccRCC samples and corresponding adjacent normal renal tissue samples by RT-qPCR analysis. As shown in Figure 1B, HCP5 was significantly enhanced in ccRCC tissue samples in contrast to the adjacent normal renal tissues ($p<0.001$). Meanwhile, we observed that the level of HCP5 was exceedingly increased in all six ccRCC cell lines compared to that in normal human renal (HK-2) cells (Figure 1C, $p<0.05$). To further explore the clinical characteristics connected with HCP5 in ccRCC, we classified 76 patients with ccRCC into two subgroups: the HCP5 high expression group (n=38) and HCP5 low expression group(n=38) according to the median value of HCP5 expression. Chi-square test showed that high HCP5 expression was sharply relevant with the tumor size ($p=0.0084$) and TNM stage ($p=0.0049$) for ccRCC patients (Table I). Besides, survival analysis indicated that the ccRCC patients with high HCP5 expression exhibited unfavorable survival prognosis with dramatically shorter PFS and OS compared to those with low HCP expression (Figure 1D and 1E, $p=0.0019$, $p=0.0104$, respectively). All together, these findings manifested that HCP5 was significantly expanded in ccRCC patients and cells and might be tightly correlated with ccRCC progression.

Downregulation of LncRNA HCP5 Repressed Cell Growth and Mobility of CcRCC In Vitro

To further explore the biological function of HCP5 in ccRCC progression, loss-of-function analysis was performed in 786-O and Caki-1 cells due to the highest expression among six ccRCC cell lines. Silenced efficiency of HCP5 was confirmed in 786-O and Caki-1 cells transfected with si-HCP5 (Figure 2A, $p<0.01$). CCK-8 assays were performed and the growth curve displayed that the knockdown of HCP5 signifi-

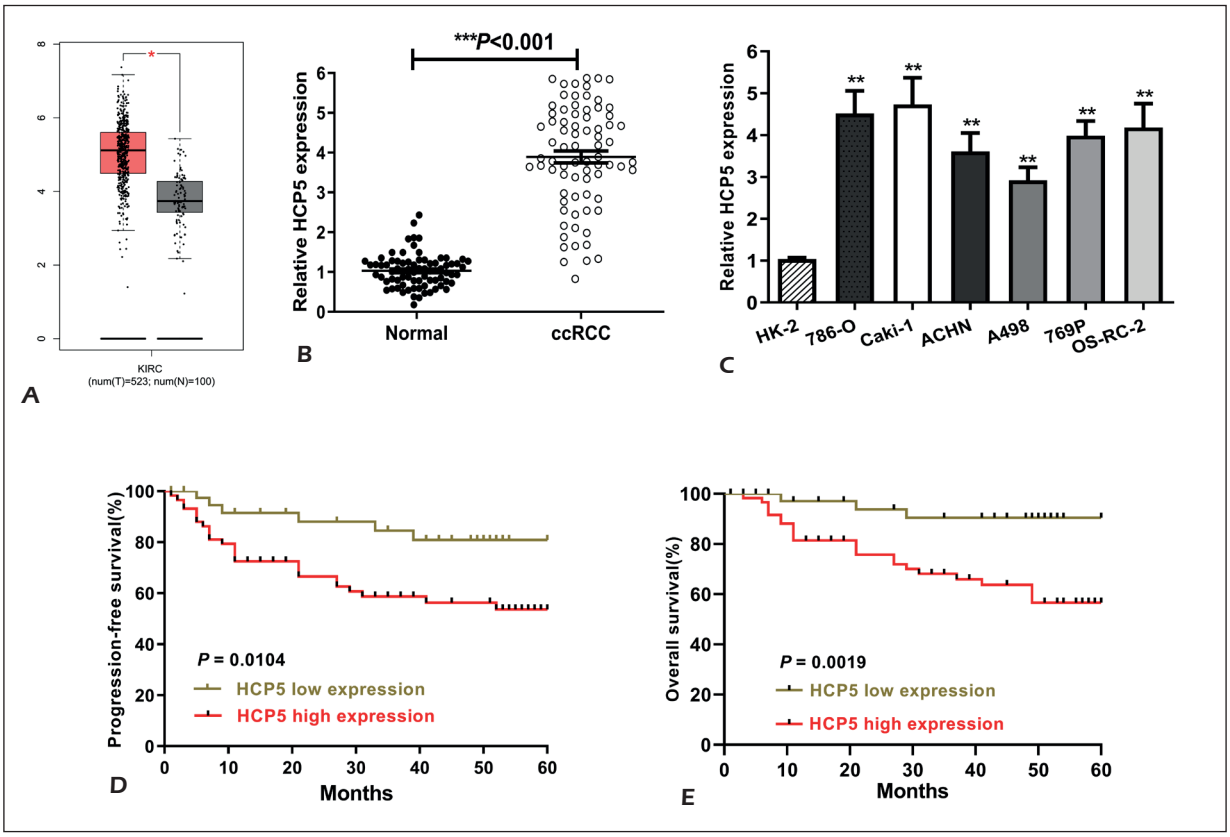

Figure 1. The expression of HCP5 in ccRCC samples was upregulated and associated with distasteful patients' prognosis. **A**, HCP5 expression prolife in ccRCC and normal tissues was obtained from the Cancer Genome Atlas (TCGA) by an online tool "GEPIA". **B**, The expression level of HCP5 was quantified in ccRCC samples and adjacent normal renal tissues from 76 pairs patients with ccRCC. **C**, Expression level of HCP5 in six ccRCC cell lines (786-O, Caki-1, ACHN, A498, 769P, OS-RC-2) and one human normal human renal cell line (HK2). **D** and **E**, The overall survival (OS) and progression-free survival (PFS) of 76 patients with ccRCC with high or low HCP5 levels was assessed. *p<0.05; **p<0.01.

Table I. Relationship between HCP5 expression and clinicopathological characteristics in patients with ccRCC.

Characteristics	Total (n=76)	HCP5 expression		*p*-value*
		High	Low	
Age (years)				
≤ 60	48	26	22	0.3415
> 60	28	12	16	
Gender				
Male	56	30	26	0.2974
Female	20	8	12	
Tumor size (cm)				
≤7	49	30	19	0.0084**
>7	27	8	19	
Fuhrman grade				
I+II	55	28	27	0.7976
III+IV	21	10	11	
Tumor stage				
pT1	40	23	17	0.1681
pT2+T3	36	15	21	
TNM stage				
I+II	60	25	35	0.0049**
III+IV	16	13	3	

**p<0.01

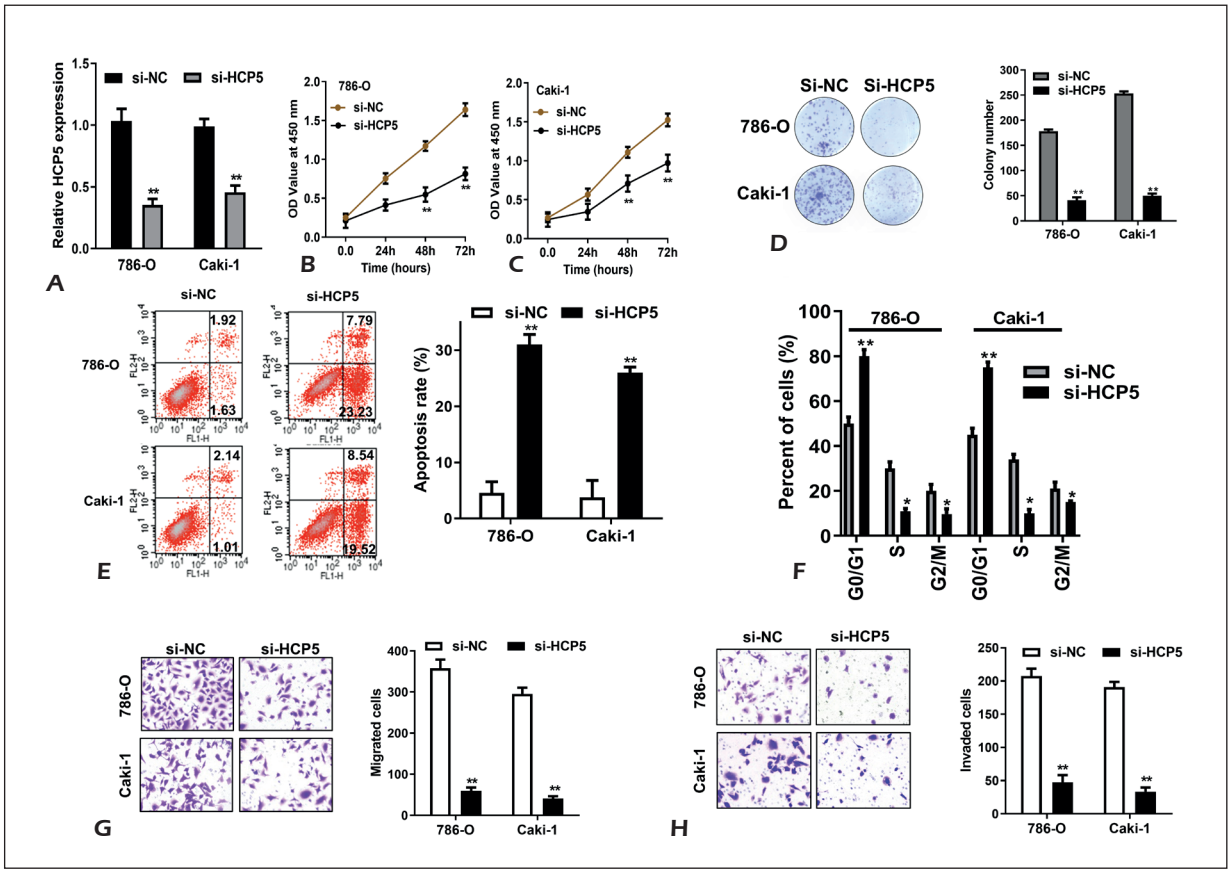

Figure 2. Silencing of HCP5 prohibited the growth, migration and invasion of ccRCC cells *in vitro*. **A**, The relative expression of HCP5 was quantified in 786-O and Caki-1 cells transfected with si-HCP5 or si-NC. **B** and **C**, Knockdown of HCP5 significantly inhibited cell proliferation of 786-O and Caki-1 cells transfected with si-HCP5 or si-NC by CCK-8 assay. **D**, Knockdown of HCP5 markedly diminished the colony-forming capacity of 786-O and Caki-1 cells transfected with si-HCP5 or si-NC (magnification 50×). **E**, Knockdown of HCP5 facilitated cell apoptosis of 786-O and Caki-1 cells after transfection with either si-HCP5 or si-NC. **F**, Knockdown of HCP5 arrested cell cycle of 786-O and Caki-1 cells transfected with si-HCP5 or si-NC at G0/G1 stage. **G** and **H**, Knockdown of HCP5 inhibited the migration and invasion of 786-O and Caki-1 cells transfected with si-HCP5 or si-NC by transwell assay; the presented pictures were captured with a 50 × magnification. *p<0.05, **p<0.01. Data were shown as mean ±SD, and all experiments were performed in triplicate.

cantly abrogated the proliferation of 786-O and Caki-1 cells (Figure 2B and 2C, p<0.01). Then, the inhibitory role of proliferation induced by the silencing of HCP5 was further validated by colony formation assays and the data showed that the 786-O and Caki-1 cells transfected with si-HCP5 formed the less colonies compared to that transfected with si-NC (Figure 2D, p<0.01). Besides, flow cytometric assay suggested that the knockdown of HCP5 led to the higher apoptotic rate in contrast with negative control (Figure 2E, p<0.01). The knockdown of HCP5 significantly increased cell proportion of G1 transition cells and reduced the proportion of G2 and S phases cells compared to the cells transfected with negative control (Figure 2F, p<0.01), indicating that the cell cycle was arrested at the G0/G1 stage. Meanwhile, transwell assays exhibited that the knockdown of HCP5 impaired the migratory and invasive ability of 786-O and Caki-1 cells in contrast with that in cells transfected with negative control (Figure 2G and 2H, p<0.01). Altogether, the knockdown of HCP5 strongly suppressed the growth and mobility of ccRCC *in vitro*.

HCP5 Served as a Sponge for MiR-140-5p

It has been reported that lncRNAs can regulate the expression of target gene by combining with some specific miRNAs in the cellular cytoplasm or by interplaying with RNA binding proteins in cell nucleus[27]. Then, we detected the location of HCP5 in 786-O and Caki-1 cells by nuclear/cytoplasmic fractionation assay and the results suggested that HCP5 was pre-

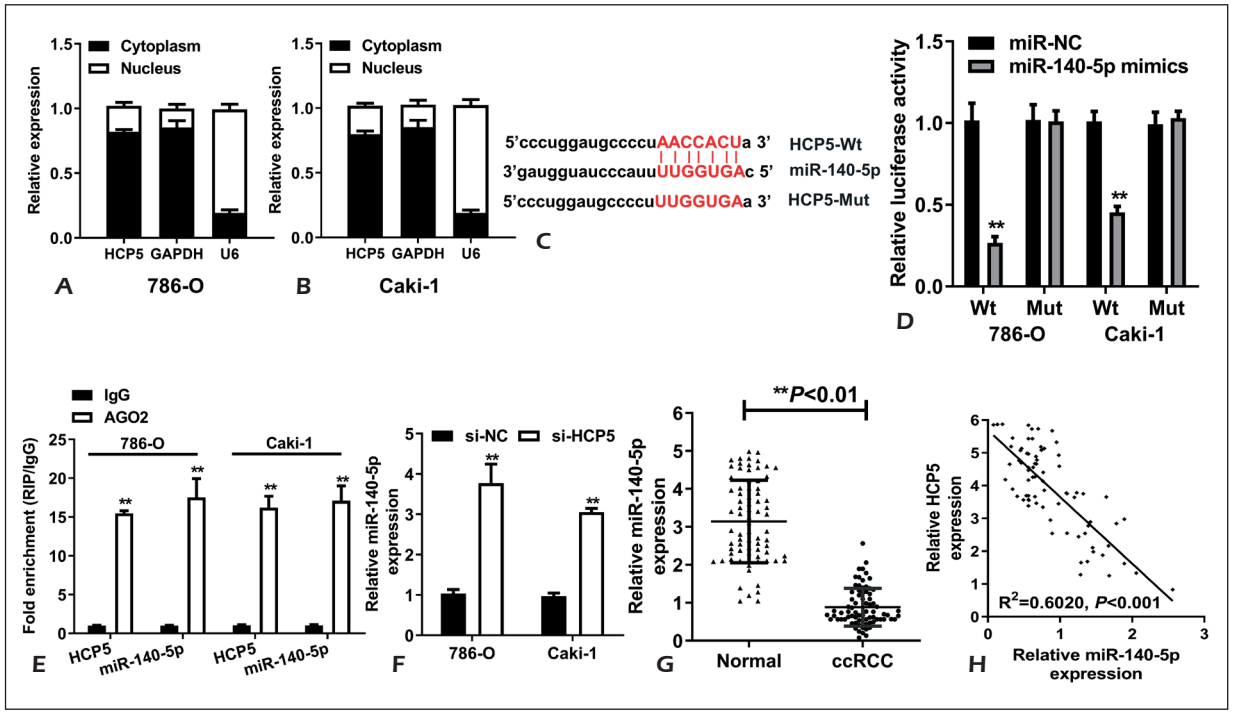

Figure 3. HCP5 acted as the molecular sponge of miR-140-5p in ccRCC cells. **A** and **B**, HCP5 was prominently located in the cytoplasm of ccRCC cells. **C**, The binding sites between HCP5 and miR-140-5p were predicted by bioinformatic analysis. The mutant binding site of HCP5 was also exhibited. **D**, Dual-luciferase reporter assay was performed in the 786-O and Caki-1 cells transfected with miR-140-5p mimics to detect the luciferase activity of the HCP5-Wt and HCP5-Mut. **E**, ARIP assay indicated that both HCP5 and miR-140-5p were concentrated in Ago2 containing beads. **F**, The relative expression of miR-140-5p were measured in 786-O and Caki-1 cells transfected with si-HCP5 or si-NC. **G**, The expression of miR-140-5p in ccRCC samples were predominantly decreased compared to matched adjacent normal renal tissue samples. **H**, Strong negative relationship between miR-140-5p and HCP5 expression in ccRCC tissues was analyzed by Spearman's correlation analysis. $^{**}p<0.01$. Data were shown as mean ±SD, and all experiments were performed in triplicate.

dominantly enriched in the cytoplasm of 786-O and Caki-1 cells (Figure 3A and 3B), indicating that HCP5 might serve as ceRNA by sponging a miRNA in ccRCC. Subsequently, the bioinformatic website StarBase V3.0 analysis found that HCP5 harboured an assumed binding site for miR-140-5p (Figure 3C). The Luciferase reporter assay further confirmed the binding relationship between HCP5 and miR-140-5p (Figure 3D, $p<0.01$). Besides, the RIP assay utilizing the antibody against Ago2 also validated the direct interaction between HCP5 and miR-140-5p in 786-O and Caki-1 cells, which indicated that miR-140-5p was an HCP5-targeted miRNA (Figure 3E, $p<0.01$). What's more, miR-140-5p expression showed an increasing trend in ccRCC cells after inhibition of HCP5 expression in 786-O and Caki-1 cells (Figure 3F, $p<0.01$). Then, we observed that miR-140-5p was significantly abrogated in ccRCC tissue samples relative to adjacent normal renal tissues (Figure 3G, $p<0.01$), which suggested that miR-140-5p might function as a tumor-suppressive gene. In addition, Spearman's correlation analysis identified a negative expression correlation between HCP5 and miR-140-5p (Figure 3H; $R^2=0.6020$, $p<0.001$). All in all, these data presented competent proof to demonstrate that HCP5 straightly sponged miR-140-5p in ccRCC cells.

IGF1R Was a Direct Target Gene of MiR-140-5p in CcRCC Cells

To further explore the target gene of miR-140-5p in ccRCC, we used online bioinformatic databases (TargetScan, microRNA) to search the putative targets of miR-140-5p. To our interest, IGF1R was observed to be a major target of miR-140-5p based on two bioinformatics databases (Figure 4A), and IGF1R has been constantly reported to participate in the growth, angiogenesis and metabolism of ccRCC[24]; therefore, in the future study, we will focuse on IGF1R. According to this inference, we performed the Luciferase reporter assays and confirmed that

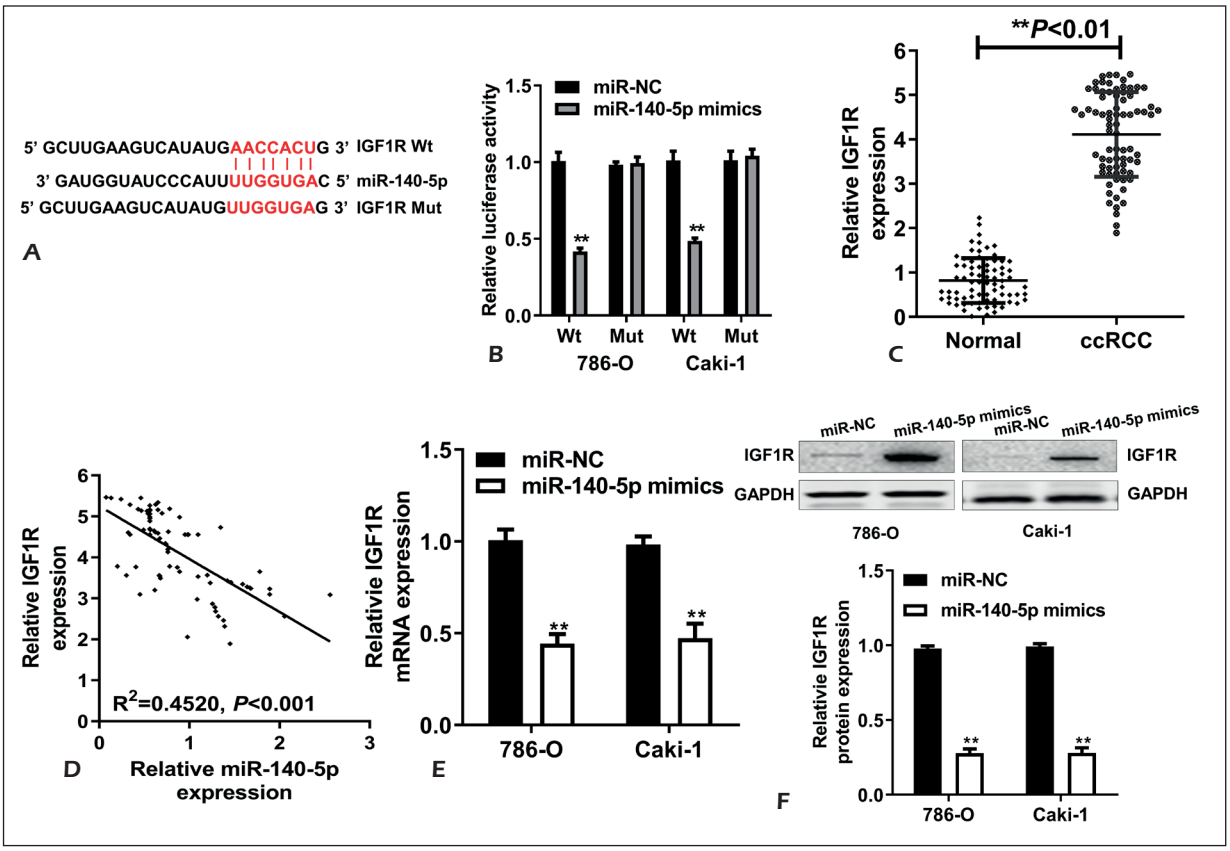

Figure 4. IGF1R was the target of miR-140-5p in ccRCC. **A**, The binding sequence of miR-140-5p to HCP5 3'UTR was assessed by bioinformatic database. **B**, The relative Luciferase activity of reporters harboring the IGF1R-Wt or IGF1R-Mut in 786-O and Caki-1 cells transfected with miR-140-5p mimics. **C**, The expression of IGF1R in ccRCC samples and matched adjacent normal renal samples. **D**, Strong negative association between miR-140-5p and IGF1R in ccRCC samples was evaluated by Spearman's correlation analysis. **E**, The relative mRNA expression of IGF1R was detected in 786-O and Caki-1 cells transfected with miR-140-5p mimics or miR-NC. **F**, The relative protein expression of IGF1R was detected in 786-O and Caki-1 cells transfected with miR-140-5p mimics or miR-NC. $^{**}p<0.01$. Data were shown as mean ±SD, and all experiments were performed in triplicate.

the repression of Luciferase activity was diminished in 786-O and Caki-1 cells contransfected with the miR-140-5p mimics and mutant IGF1R 3'-UTR (Figure 4B, $p<0.01$). Moreover, the IGF1R mRNA level was significantly decreased in ccRCC tissue samples compared to adjacent normal renal tissues by qRT-PCR analysis (Figure 4C, $p<0.01$). A significantly inverse correlation between miR-140-5p and IGF1R mRNA levels among these 76 ccRCC tissue samples was also observed by Spearman's correlation analysis (Figure 4D; $R^2=0.4520$, $p<0.001$). Additionally, the overexpressed expression of miR-140-5p significantly suppressed IGF1R in 786-O and Caki-1 cells at both the mRNA (Figure 4E, $p<0.01$) and protein (Figure 4F, $p<0.01$) levels. In short, these data implied that IGF1R was a direct target of miR-140-5p in ccRCC cells.

Mir-140-5p/IGF1R Mediated Oncogenic Roles of HCP5 in ccRCC Cells

Since lncRNA HCP5 could sponge to miR-140-5p, which could regulate the expression of IGF1R, we wondered whether HCP5 could indirectly regulate the expression of IGF1R by miR-140-5p. Restored experiments were performed introducing the miR-140-5p inhibitor into cells of HCP5 knockdown. Remarkably, an enhancement of IGF1R 3'-UTR activity (Figure 5A, $p<0.01$) in HEK-293 cells and a reduction in the IGF1R mRNA (Figure 5B, $p<0.01$) and protein amount (Figure 5C, $p<0.01$) in 786-O and Caki-1 cells, as a result of HCP5 knockdown, were countered when the miR-140-5p inhibitor was contransfected. The recovery of IGF1R by the mediation of miR-140-5p inhibitor inhibited the effects of the HCP5 silencing on 786-O and Caki-1 cells pro-

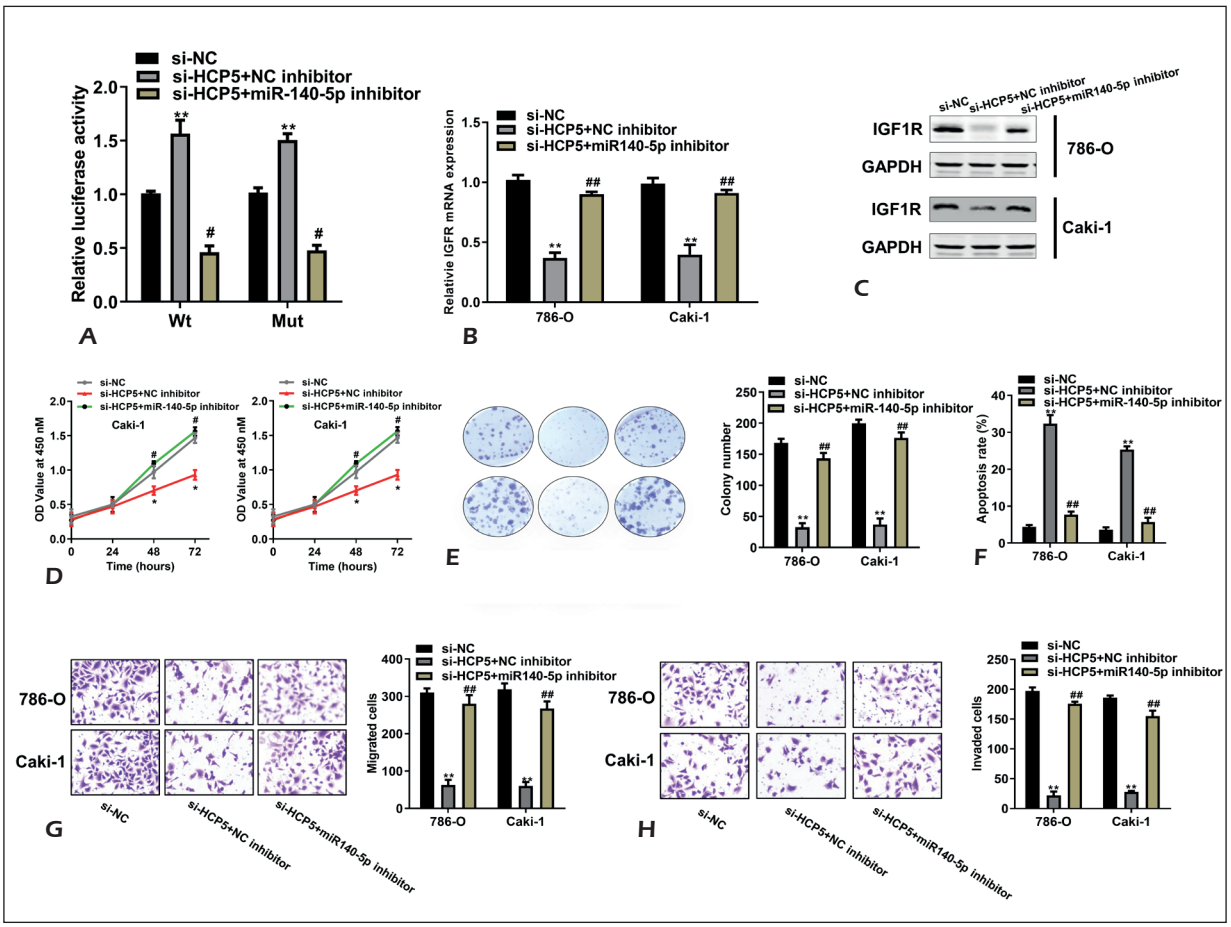

Figure 5. IGF1R was positively regulated by HCP5 and knockdown of miR-140-5p expression neutralized the effects of the HCP5 silencing on ccRCC cells. **A**, The Luciferase activity was detected in HEK-293 cells co-transfected with si-HCP5 or miR-140-5p inhibitor and IGF1R 3'-UTR for 48 h. **B** and **C**, The downregulated miR-140-5p decreased the mRNA and protein expression of IGF1R in 786-O and Caki-1 cells transfected with si-HCP5. **D**, MiR-140-5p could distinctly antagonize the suppressive effects of HCP5 silencing on proliferation of ccRCC cells. **E**, MiR-140-5p partially rescued the capability of the colony formation in HCP5 silencing ccRCC cells (magnification 50×). **F**, MiR-140-5p partially abolished the elevation of apoptosis in HCP5 silencing ccRCC cells. **G** and **H**, MiR-140-5p partially inverted the repressive outcomes of HCP5 on migration and invasion of ccRCC cells (magnification 50×). $^{**}p<0.01$, compared to si-NC; $^{\#}p<0.05$, compared to si-HCP5 + NC inhibitor. Data were shown as mean ±SD, and all experiments were performed in triplicate.

liferation (Figure 5D, $p<0.01$), colony formation (Figure 5E, $p<0.01$), apoptosis (Figure 5F, $p<0.01$), migration (Figure 5G, $p<0.01$), and invasion (Figure 5H, $p<0.01$). Taken together, the HCP5 could act oncogenic role by miR-140-5p/IGF1R axis in ccRCC cells.

The Downregulation of HCP5 Inhibited CcRCC Tumor Growth In Vivo

786-O cells transfected with either si-HCP5 or si-NC were subcutaneously inoculated into the back flank of nude mice. Consistent with the *in vitro* results, the tumor volume was significantly diminished in the si-HCP5 group compared to the si-NC group (Figure 6A and 6B, $p<0.01$). Additionally, xenograft tumors were harvested and weighed after the nude mice were mercy killing. The HCP5-knockdown xenografts displayed prominent tumor weight impairment compared with the si-NC group (Figure 6C, $p<0.01$). Besides, HCP5 and miR-140-5p expression in the tumor xenografts derived from si-HCP5-transfected 786-O cells were measured by the qRT-PCR analysis. HCP5 expression was observed to be reduced (Figure 6D, $p<0.01$), whereas miR-140-5p expression was enlarged (Figure 6E, $p<0.01$). Similarly, IGF1R was sharply down-regulated in the si-HCP5 group compared with the si-NC group (Figure 6F) by Western blot analysis. All together, these data demonstrated that the down-

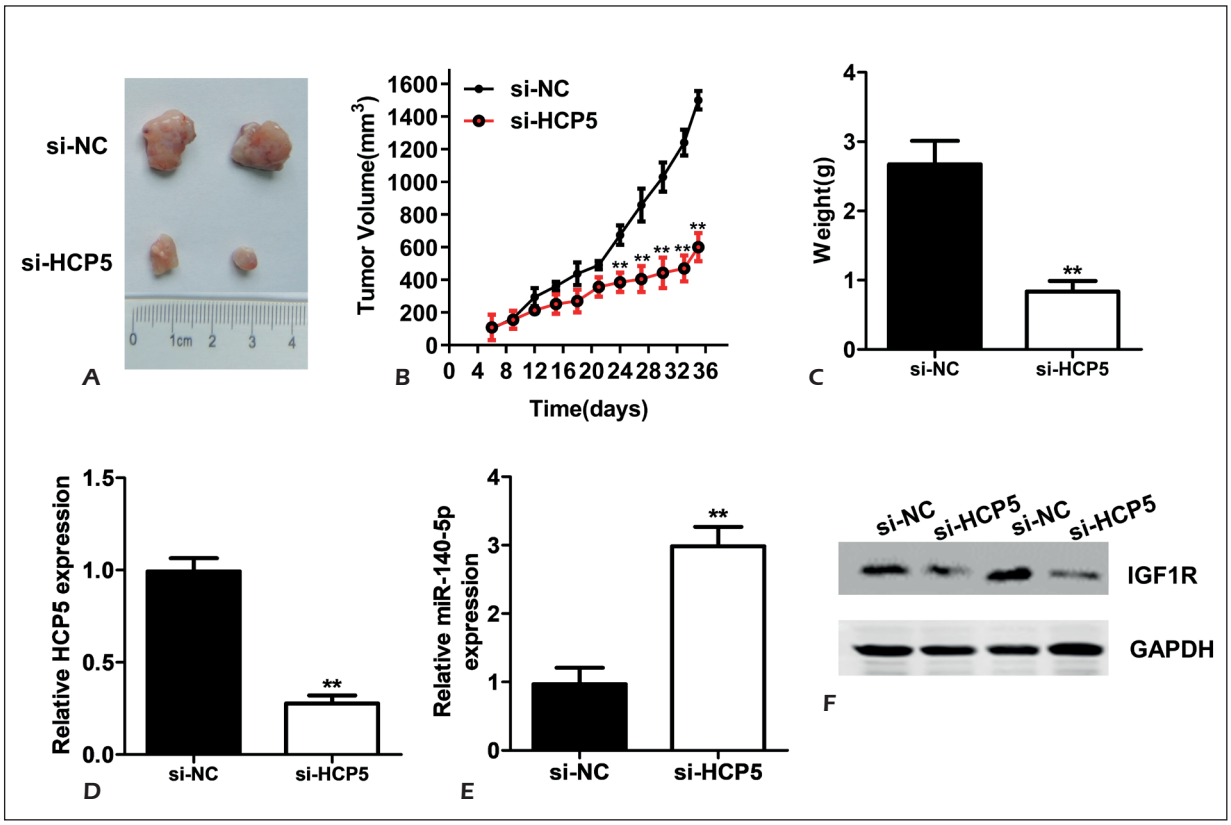

Figure 6. Knockdown of HCP5 expression suppressed growth of ccRCC xenograft tumor in vivo. **A**, Representative photograph of xenograft tumors derived from si-HCP5 transfected or si-NC-transfected 786-O cells. **B**, Tumor volumes were calculated as the length × width2 × 0.5 every 3 days after injection. **C**, The mean weight of tumor xenografts was measured after the tumors were harvested. **D** and **E**, qRT-PCR analysis of HCP5 and miR-140-5p expression in xenograft tumors tissues. **F**, Protein expression of IGF1R in the xenografts of si-HCP5 and si-NC groups was measured by Western blotting. **$p<0.01$ *vs.* the si-NC group.

regulation of HCP5 could attenuate the tumor growth of ccRCC *in vivo* by regulating the miR-140-5pIGF1R axis.

Discussion

LncRNAs can induce the abnormal growth and metastasis of ccRCC by regulating the expression of target gene. These studies allow us to explore the mechanism of the initial and progression of ccRCC to develop better strategies for the treatment of this disease. Li et al[28] reported that long noncoding RNA MRCCAT1 promoted metastasis of clear cell renal cell carcinoma via inhibiting NPR3 and activating p38-MAPK signaling. Zhang et al[29] found that lncRNA SNHG3 promoted clear cell renal cell carcinoma proliferation and migration by upregulating TOP2A. Song et al[30] revealed that lncRNA ADAMTS9-AS2 inhibited cell proliferation and decreased chemoresistance in clear cell renal cell carcinoma via the miR-27a-3p/FOXO1 axis. Although HCP5 has been reported to be overexpressed and promotes the progression in many human malignancies, the role of HCP5 is still unclear and needs further exploration in ccRCC.

In this research, we found that the expression of lncRNA HCP5 was potently upregulated compared with the adjacent non-tumor tissues. Similarly, the expression of HCP5 was also upregulated in ccRCC cancer cell lines compared with the normal renal cell. Moreover, high-level expression of HCP5 was related with dismal clinicopathological characteristics and worse survival prognosis. Additionally, functional assays uncovered that the knockdown of HCP5 expression suppressed ccRCC cell proliferation and the colony formation ability, induced G0-G1 cell cycle arrest, sparked apoptosis, inhibited cell migration and invasion *in vitro*,

and prohibited growth of xenografts *in vivo*. Consistently with previous reports of other cancers, our data provided evidence for HCP5 as an oncogene, as well as the prognostic factor in ccRCC.

However, how lncRNA HCP5 performed its oncogenic actions in ccRCC by molecular event remained to be explored. LncRNA-miRNA-mRNA ceRNA network has been demonstrated to regulate the expression of target mRNA by competing with miRNAs[27]. In this study, we disclosed that HCP5 functioned as a direct target of miR-140-5p in ccRCC by bioinformatics tools, Luciferase assay, and RNA immunoprecipitation. MiR-140-5p is significantly decreased and inhibits the progression of many neoplasms, including gastric cancer, breast cancer, chronic myeloid leukemia, retinoblastoma, and lung cancer[19-23]. However, the expression and function of miR-140-5p in ccRCC have yet been investigated. Consistently, we found that the expression of miR-140-5p was significantly downregulated in ccRCC tissues. The data indicated miR-140-5p might act as one suppressor in ccRCC, which should be explored in the future study. We also observed that miR-140-5p expression was inversely associated with HCP5 expression in ccRCC tissues. What's more, silencing of HCP5 dramatically boosted the expression of miR-140-5p. Meanwhile, miR-140-5p inhibitor could partially counteract the biological function to the silencing of HCP5. So, HCP5 acted its oncogenic effects on ccRCC cells by sponging miR-140-5p.

MiRNAs exert its effects through straightly binding to the 3'-UTRs of their target mRNAs[31]. Bioinformatics analysis and Luciferase reporter assay indicated that the 3'-UTR of IGF1R matched the seed sequence of miR-140-5p and could be directly targeted by miR-140-5p. In addition, IGF1R was augmented in ccRCC tissues, displaying an inverse association with miR-140-5p expression. At the same time, we also observed that IGF1R mRNA and protein levels were decreased by miR-140-5p in ccRCC cells. These results collectively validate IGF1R as a direct target gene of miR-140-5p in ccRCC. Finally, we found that HCP5 sponged miR-140-5p to promote IGF1R expression in ccRCC *in vitro* and *in vivo*. Subsequently, rescued experiments confirmed that HCP5 exerted its oncogenic effects in an IGF1R-dependent manner.

Conclusions

We evidently indicated that lncRNA HCP5 was a prognostic biomarker in ccRCC, which was closely related with adverse clinical characteristics and poor survival. Furthermore, knockdown of HCP5 could effectively abrogate cell proliferation and migration by targeting the miR-140-5p/IGF1R axis *in vitro* and *in vivo*, illuminating a potential therapeutic target for HCP5 in ccRCC treatment.

Conflict of Interests

The authors declare that they have no conflict of interests.

References

1) Siegel RL, Miller KD, Jemal A. Cancer statistics, 2019. CA Cancer J Clin 2019; 69: 7-34.
2) Capitanio U, Montorsi F. Renal cancer. Lancet 2016; 387: 894-906.
3) Cairns P. Renal cell carcinoma. Cancer Biomark 2010; 9: 461-473.
4) Barata PC, Rini BI. Treatment of renal cell carcinoma: current status and future directions. CA Cancer J Clin 2017; 67: 507-524.
5) Bhan A, Soleimani M, Mandal SS. Long noncoding RNA and cancer: a new paradigm. Cancer Res 2017; 77: 3965-3981.
6) Jiang MC, Ni JJ, Cui WY, Wang BY, Zhuo W. Emerging roles of lncRNA in cancer and therapeutic opportunities. Am J Cancer Res 2019; 9: 1354-1366.
7) Sanchez Calle A, Kawamura Y, Yamamoto Y, Takeshita F, Ochiya T. Emerging roles of long non-coding RNA in cancer. Cancer Sci 2018; 109: 2093-2100.
8) Xu H, Zhao G, Zhang Y, Jiang H, Wang W, Zhao D, Yu H, Qi L. Long non-coding RNA PAXIP1-AS1 facilitates cell invasion and angiogenesis of glioma by recruiting transcription factor ETS1 to upregulate KIF14 expression. J Exp Clin Cancer Res 2019; 38: 486.
9) Zhang Y, Yuan Y, Zhang Y, Cheng L, Zhou X, Chen K. SNHG7 accelerates cell migration and invasion through regulating miR-34a-Snail-EMT axis in gastric cancer. Cell Cycle 2020; 19: 142-152.
10) Jin Y, Xie H, Duan L, Zhao D, Ding J, Jiang G. Long non-coding RNA CASC9 and HIF-1a form a positive feedback loop to facilitate cell proliferation and metastasis in lung cancer. Onco Targets Ther 2019; 12: 9017-9027.
11) Liu Y, Wang J, Dong L, Xia L, Zhu H, Li Z, Yu X. Long noncoding RNA HCP5 regulates pancreatic cancer gemcitabine (GEM) resistance by sponging hsa-miR-214-3p to target HDGF. Onco Targets Ther 2019; 12: 8207-8216.
12) Wei X, Gu X, Ma M, Lou C. Long noncoding RNA HCP5 suppresses skin cutaneous melanoma development by regulating RARRES3 gene expression via sponging miR-12. Onco Targets Ther 2019; 12: 6323-6335.
13) Wang L, Luan T, Zhou S, Lin J, Yang Y, Liu W, Tong X, Jiang W. LncRNA HCP5 promotes triple negative breast cancer progression as a ceRNA to regulate

BIRC3 by sponging miR-219a-5p. Cancer Med 2019; 8: 4389-4403.

14) Jiang L, Wang R, Fang L, Ge X, Chen L, Zhou M, Zhou Y, Xiong W, Hu Y, Tang X, Li G, Li Z. HCP5 is a SMAD3-responsive long non-coding RNA that promotes lung adenocarcinoma metastasis via miR-203/SNAI axis. Theranostics 2019; 9: 2460-2474.

15) Yun WK, Hu YM, Zhao CB, Yu DY, Tang JB. HCP5 promotes colon cancer development by activating AP1G1 via PI3K/AKT pathway. Eur Rev Med Pharmacol Sci 2019; 23: 2786-2793.

16) Yang C, Sun J, Liu W, Yang Y, Chu Z, Yang T, Gui Y, Wang D. Long noncoding RNA HCP5 contributes to epithelial-mesenchymal transition in colorectal cancer through ZEB1 activation and interacting with miR-139-5p. Am J Transl Res 2019; 11: 953-963.

17) Zhao W, Li L. SP1-induced upregulation of long non-coding RNA HCP5 promotes the development of osteosarcoma. Pathol Res Pract 2019; 215: 439-445.

18) Liang L, Xu J, Wang M, Xu G, Zhang N, Wang G, Zhao Y. LncRNA HCP5 promotes follicular thyroid carcinoma progression via miRNAs sponge. Cell Death Dis 2018; 9: 372.

19) Nie ZY, Liu XJ, Zhan Y, Liu MH, Zhang XY, Li ZY, Lu YQ, Luo JM, Yang L. MiR-140-5p induces cell apoptosis and decreases Warburg effect in chronic myeloid leukemia by targeting SIX1. Biosci Rep 2019; 39. pii: BSR2019015020.

20) Liao Y, Yin X, Deng Y, Peng X. MiR-140-5p suppresses retinoblastoma cell growth via inhibiting c-Met/AKT/mTOR pathway. Biosci Rep 2018; 38. pii: BSR20180776.

21) Zhang JR, Zhu RH, Han XP. MiR-410 affects the proliferation and apoptosis of lung cancer A549 cells through regulation of SOCS3/JAK-STAT signaling pathway. Eur Rev Med Pharmacol Sci 2018; 22: 5994-6001.

22) Fang Z, Yin S, Sun R, Zhang S, Fu M, Wu Y, Zhang T, Khaliq J, Li Y. MiR-140-5p suppresses the proliferation, migration and invasion of gastric cancer by regulating YES1. Mol Cancer 2017; 16: 139.

23) Lu Y, Qin T, Li J, Wang L, Zhang Q, Jiang Z, Mao J. MicroRNA-140-5p inhibits invasion and angiogenesis through targeting VEGF-A in breast cancer. Cancer Gene Ther 2017; 24: 386-392.

24) Tracz AF, Szczylik C, Porta C, Czarnecka AM. Insulin-like growth factor-1 signaling in renal cell carcinoma. BMC Cancer 2016; 16: 453.

25) Xu MD, Wang Y, Weng W, Wei P, Qi P, Zhang Q, Tan C, Ni SJ, Dong L, Yang Y, Lin W, Xu Q, Huang D, Huang Z, Ma Y, Zhang W, Sheng W, Du X. A positive feedback loop of lncRNA-PVT1 and FOXM1 facilitates gastric cancer growth and invasion. Clin Cancer Res 2017; 23: 2071-2080.

26) Wang Z, Yang B, Zhang M, Guo W, Wu Z, Wang Y, Jia L, Li S, Cancer Genome Atlas Research N, Xie W, Yang D. LncRNA epigenetic landscape analysis identifies EPIC1 as an oncogenic lncRNA that interacts with MYC and promotes cell-cycle progression in cancer. Cancer Cell 2018; 33: 706-720. e709.

27) Slack FJ, Chinnaiyan AM. The role of non-coding RNAs in oncology. Cell 2019; 179: 1033-1055.

28) Li JK, Chen C, Liu JY, Shi JZ, Liu SP, Liu B, Wu DS, Fang ZY, Bao Y, Jiang MM, Yuan JH, Qu L, Wang LH. Long noncoding RNA MRCCAT1 promotes metastasis of clear cell renal cell carcinoma via inhibiting NPR3 and activating p38-MAPK signaling. Mol Cancer 2017; 16: 111.

29) Zhang C, Qu Y, Xiao H, Xiao W, Liu J, Gao Y, Li M, Liu J. LncRNA SNHG3 promotes clear cell renal cell carcinoma proliferation and migration by upregulating TOP2A. Exp Cell Res 2019; 384: 111595.

30) Song EL, Xing L, Wang L, Song WT, Li DB, Wang Y, Gu YW, Liu MM, Ni WJ, Zhang P, Ma X, Zhang X, Yao J, Chen Y, An RH. LncRNA ADAMTS9-AS2 inhibits cell proliferation and decreases chemoresistance in clear cell renal cell carcinoma via the miR-27a-3p/FOXO1 axis. Aging (Albany NY) 2019; 11: 5705-5725.

31) Reddy KB. MicroRNA (miRNA) in cancer. Cancer Cell Int 2015; 15: 38.